

Fast-Food Sequelae from Hepatic Steatosis to Dysplasia in Inactive Adult Male Mice Highlighting Endoplasmic Reticulum Stress and Cytochrome-P450-2-E1 Roles and Recovery Possibility

Abeer Ibraheem Omar, Marwa Mohamed Yousry and Eman Abas Farag

Department of Histology, Faculty of Medicine, Cairo University, Cairo, Egypt

ABSTRACT

Introduction: Globally, non-alcoholic fatty liver disease (NAFLD) is a common cause of chronic liver disease. It occurs in 20-40% of the population and 70-95% of diabetic and obese patients. NAFLD could progress from steatosis to non-alcoholic steatohepatitis (NASH). Worldwide, fast-food diet (FFD) is widely used due to its convenience and palatability.

Aim of Work: This study aimed at evaluating the hepatic biochemical, histological, and morphometric changes occurred on persistent FFD and sedentary lifestyle in adult male mice, the possibility of premalignant dysplastic changes and the recovery potentiality after FFD discontinuation. Moreover, the possible roles of endoplasmic reticulum (ER) stress and cytochrome-P450-family2-subfamilyE-gene1 (CYP2E1) were assessed.

Materials and Methods: 48 adult male mice were kept singly in cages and grouped into control, FFD and recovery groups. Each group was furtherly divided according to the time of sacrifice. 3 control subgroups with FFD subgroups were sacrificed at 4, 6&8 months. However, the remaining 3 control subgroups with the recovery subgroups were sacrificed at 6, 8&10 months. Biochemical, histological, and morphometric studies were done.

Results: FFD group showed progressive hepatic lesion from accumulation of fat microvesicles to deposition of macrovesicles with ER stress, unfolded protein response (UPR) activation, CYP2E1 over-expression, inflammation & apoptosis. Then, there was development of multiple small dysplastic foci inside the lesion area. The improvement in the recovery group was significant in case of steatosis, non-significant in case of NASH and undetectable in dysplasia.

Conclusion: Chronic FFD with sedentary lifestyle could lead to hepatic steatosis and sequentially to NASH through ER stress, UPR activation and CYP2E1 over-activation. With persistence of FFD and inactive behavior, the insult might progress to dysplasia, a precancerous lesion. Although more time is needed for appropriate assessment of recovery, it could be assumed that hepatic steatosis is easily recoverable, NASH is poorly recoverable while dysplasia is irrecoverable.

Received: 27 December 2021, **Accepted:** 27 January 2022

Key Words: CYP2E1, ER-stress, FFD, NAFLD, UPR.

Corresponding Author: Abeer Ibraheem Omar, MD, Department of Histology, Faculty of Medicine, Cairo University, Cairo, Egypt, **Tel.:** +20 10 0259 6677, **E-mail:** kaboree2002@gmail.com

ISSN: 1110-0559, Vol. 46, No. 2

INTRODUCTION

Hepatocellular carcinoma (HCC) represents the 7th widespread malignant tumor and the 2nd cause of tumor deaths all over the world^[1]. Few of its patients can receive potentially therapeutic treatment but with great frequency of recurrence^[2].

Denovo HCC could rarely happen, but it usually develops as a result of a complicated multiphasic process^[3] whose steps are not completely recognized. Tendency for development of different forms of HCC have increased following chronic inflammatory and fibrotic liver diseases as hepatitis C, metabolic diseases such as alcoholic fatty liver and congenital diseases like hemochromatosis^[4]. This tendency is explained by the abnormal regeneration of the altered hepatocytes forming premalignant dysplastic lesions that have a high prevalence for malignant transformation^[3].

Worldwide, non-alcoholic fatty liver disease (NAFLD) affects 20-40% of the population and 70-95% of type II diabetic patients and obese people^[5]. It is considered as the supreme cause of chronic hepatic insults^[6] where it

starts with a state of metabolic dysfunction called hepatic steatosis with extreme accumulation of lipid droplets in the hepatocytes' cytoplasm^[7]. Such metabolic problem could progress to non-alcoholic steatohepatitis (NASH)^[8].

High fat diet (HFD) is proved to increase the fat in the liver cells to the limit exceeding the capacity of the liver to metabolize them. This leads to hepatic intracellular fat accumulation (hepatic steatosis)^[9] and consequent NASH^[10]. Till now there is no approved definite treatment for both NAFLD and NASH^[6,11].

Fast-food diet (FFD), also called Western diet (WD) or Cafeteria diet, is concerned with the rapidly cooked and served food available at different locations such as sit-down restaurants, take-away, drive-thru and delivery. It is well-liked as it is economical, convenient, and palatable. Such kind of food is abundant in saturated fats, cholesterol, and fructose in the soft drinks^[12,13]. This contrasts with HFD which is rich mainly in unsaturated fats^[10].

Endoplasmic reticulum (ER) stress is altered ER homeostasis induced by the presence of intraluminal

unfolded or misfolded newly synthesized proteins. It results in activation of an intracellular stress signaling called unfolded protein response (UPR)^[14] to restore ER homeostasis through balancing between the load of the newly synthesized proteins on ER and its capability to fold them. UPR is composed of three arms which are ER trans-membrane proteins named inositol-requiring transmembrane kinase and endonuclease 1 α (IRE1 α), double-stranded RNA (dsRNA)-dependent protein kinase-like ER kinase (PERK) and activating transcription factor-6 (ATF-6). These arms are inactive in normal conditions and get activated and over-expressed by ER stress^[15]. Such activation, based on the degree of ER stress and the continuation of the precipitating causes, may lead to one of three responses: adaptive, alarm or apoptosis^[15].

Cytochrome-P450-family2-subfamilyE-gene1 (CYP2E1) is a member of cytochrome-P450 enzyme superfamily present mainly in the hepatocytes as a membrane protein in ER, mitochondria, Golgi body, cell membrane and microsomes^[16]. Recently, its expression by the healthy sinusoidal endothelial cells (SECs) was documented^[17]. CYP2E1 is responsible for ω -1 hydroxylation of the saturated fatty acids^[18] as an alternative metabolic pathway to their β -oxidation in the mitochondria and peroxisomes^[19,20].

This study aimed at evaluating the biochemical, histological, and morphometric changes occurred in the liver of adult male mice on persistent FFD and sedentary behavior, in addition to the possibility of premalignant dysplastic changes and the possible roles of ER stress and CYP2E1. This was accompanied by assessing the potentiality of reversing these changes by discontinuation of FFD.

MATERIAL AND METHODS

Experimental Design

Forty-eight adult male mice (~30 g) were housed in the Laboratory Animal House Unit of Kasr Al-Aini, Faculty of Medicine, Cairo University according to the guidelines reported by Cairo University-Institutional Animal Care and Use Committee (CU-IACUC) (approval number CU/III/F/54/20). They were kept under the same environmental conditions for 48 hours before starting the experiment for acclimation and avoid the stress-induced dietary changes. They were housed at $24 \pm 1^\circ\text{C}$ in normal light/dark cycle and provided with ordinary chow (OC) [supplies 13% of energy as fat and composed of nearly 5% total fats from which: 0.93% saturated fatty acids (SFAs), 0.99% monounsaturated fatty acids (MUFAs), 2.2% polyunsaturated fatty acids (PUFAs) and 0.14% cholesterol^[10] and water ad libitum. With the beginning of the experiment, each mouse was kept singly in a separate cage to allow for sedentary lifestyle. Then, the total number of mice were divided equally into three main groups:

Group I (control group, 18 mice): The mice continued on OC and water ad libitum. They were furtherly classified

into subgroups Ia1, Ib1 & Ic1 (3 mice each) to be sacrificed with the corresponding subgroups of group II at 4, 6 & 8 months, in addition to subgroups Ia2, Ib2 & Ic2 (3 mice each) to be sacrificed with the three subgroups of group III at 6, 8 & 10 months.

Group II (FFD group, 15 mice): The mice, through the whole experimental duration, were provided with FFD (5342-AIN-76A Western Diet, Test Diet) that provides 40% of energy as fat and composed of about 20% total fats from which: 12.09% SFAs, 4.61% MUFAs, 0.58% PUFAs and 2% cholesterol. In addition, high-fructose corn syrup (23.1%) was added to their drinking water^[10]. These mice were equally subdivided into 3 subgroups (IIa, IIb & IIc) according to their time of sacrifice (4, 6 & 8 months).

Group III (recovery group, 15 mice): The animals were subdivided into 3 equal subgroups (IIIa, IIIb & IIIc). The mice of each subgroup were fed on FFD for 4, 6 & 8 months, respectively, followed by 2 months of OC then sacrificed i.e., subgroups IIIa, IIIb & IIIc were sacrificed at the end of the 6th, 8th & 10th months, correspondingly.

Animal studies

Serological Study

Blood samples from the tail veins of the mice in each subgroup were obtained just before their sacrifice. The samples were used to measure one of the serum hepatic enzymes (aspartate transaminase [AST]).

Animals sacrifice

At each time point for each subgroup, the animals' body weight was measured. Then the animals were sacrificed after being anesthetized with IP injection of ketamine (87 mg/kg)/xylazine (13 mg/kg)^[21], at the Laboratory Animal House Unit of Kasr Al-Aini. The abdomens were opened, and the livers were dissected and weighed. Three slices (2-2.5 mm in thickness) from the left lobe of each liver were cut (one for quantitative real-time polymerase chain reaction [qRT-PCR] and hepatic homogenates preparation, one for Paraffin block preparation and one for resin block preparation).

Quantitative real-time polymerase chain reaction (qRT-PCR)^[22]

It was done to detect relative mRNA expression of ATF-6 (an example for UPR activation markers): After total RNA extraction and complementary DNA (cDNA) synthesis, qRT-PCR of the studied genes was done using Rotor Gene 6000 series software version 1.7 (Corbett Life Science, USA) and the primers. Then the results were expressed as a normalized ratio. The PCR primer sequences used were ATF-6 (forward: 5'-TGGGAGTGAGCTGCAAGTGT-3'; reverse: 5'-ATAAGGGGAACCGAGGAG-3') and GAPDH [internal control] (Forward: 5'-CTCCATTCTCCACCTTTG-3'; Reverse: 5'-CTTGCTCTCAGTATCCTTGC-3').

Hepatic Homogenates

Liver homogenates were prepared based on a previous methodology^[22], then divided into 2 parts:

First part was used to measure hepatic triglycerides (TAG) and cholesterol using conventional colorimetric method (QuantiChrom TM assay kit, Hayward, USA).

Second part was used for ELISA according to the manufacturer's instructions to measure the values of:

- Tumour necrosis factor- α [TNF- α , pro-inflammatory cytokine (ab208348, abcam, USA)].
- Hydrogen peroxide [H₂O₂, oxidative stress (OS) marker (MBS3806313, MyBioSource, USA)], glutathione [GSH, antioxidant enzyme, (MBS267424, MyBioSource, USA)] and malondialdehyde [MDA, lipid peroxidation indicator, (MBS741034, MyBioSource, USA)].

Histological Study

A) Paraffin block preparation

The hepatic slices for Paraffin block preparation from all animals were fixed in 10% formol saline and kept for 24 hours then processed to Paraffin blocks. Six μ m-thick serial sections were cut and stained with:

- Hematoxylin and Eosin stain (H&E)^[23].
- Masson's trichrome stain^[24].
- Immunohistochemical staining for:
 - a. CYP2E1 [rabbit polyclonal antibody, ab28146, abcam, USA]: it is a marker for ω -1 hydroxylation of saturated fatty acids that appears as a cytoplasmic and membranous reactions.
 - b. Caspase-3 [rabbit polyclonal antibody, ab4051, abcam, USA]: it appears as a cytoplasmic reaction in the apoptotic cells.
 - c. Glypican-3 [mouse monoclonal antibody, [GPC3/863] ab216606, abcam, USA]: it is a marker for hepatic dysplasia and hepatocellular carcinoma that appears as a cytoplasmic reaction.

Avidin-biotin immunostaining technique required pretreatment^[24], that was carried out by 10 min boiling in 10 mM citrate buffer (cat no 005000) pH 6 for antigen retrieval. Sections were left to cool for 20 min at room temperature. Then, they were incubated for one hour with the primary antibodies. Immunostaining was completed using Ultravision One Detection System (cat no TL - 060- HLJ). Counterstaining was carried out using Lab Vision Mayer's hematoxylin (cat no TA- 060- MH). Negative control sections were prepared by the same process after excluding the primary antibodies. Citrate buffer, Ultravision One Detection System and Ultravision Mayer's hematoxylin were purchased from Labvision, ThermoFisher scientific, USA.

Resin block preparation

The hepatic slices for resin block preparation from all animals were cut into small fragments (0.5-1.0 mm³), prefixed in 2.5 % glutaraldehyde for 2 h then postfixed in 1% osmium tetroxide in 0.1 M phosphate buffer at pH 7.4 and 4 °C for 2 h. then, dehydration and resin embedding were done^[25]. Semithin (1 μ m) sections were cut using a Leica ultracut (UCT) (Glienicke, Berlin, Germany). The sections were stained with toluidine blue (1%) and examined by light microscope.

Morphometric study

Image analysis by Leica Qwin-500 LTD-software image analysis computer system (Cambridge, England) was done to measure the area percent of collagen fibers in Masson's trichrome-stained sections and of CYP2E1, caspase-3, and glypican-3 immuno-expression in the corresponding immunostained sections. Each of these measurements was done in ten non-overlapping random chosen fields (\times 100).

Statistical analysis^[26]

The morphometric and biochemical measurements were expressed as mean \pm standard deviation (SD). All of them were statistically analyzed using one-way analysis of variance (ANOVA) followed by "Tukey" post hoc test except for glypican-3 results where independent samples T-test was used. IBM Statistical Package for the Social Sciences (SPSS) version 21 was used for the calculations and the results were considered statistically significant when *P* value was < 0.05 .

All serological and biochemical studies were done at Biochemistry Department, Faculty of Medicine, Cairo University. However, all histological and morphometric studies were performed at Histology Department, Faculty of Medicine, Cairo University.

RESULTS

General observations

Laziness was noticed in the mice of all subgroups during the whole experimental duration. No deaths nor abnormal behavior, rather than laziness, was witnessed in any of the experimental animals.

Similar histological and biochemical results were found in the control subgroups so, they were collectively named as control group (group I).

Animal Data

Serological Results

The serum hepatic enzyme (AST) level (Figure 1a) demonstrated significant increase in all subgroups versus the control group. In addition, there was significant increase in subgroups IIb and IIc when compared with subgroups IIa and IIb, individually. Conversely, there were significant decrease in subgroup IIIa versus subgroup IIa, non-significant decrease in subgroup IIIb versus subgroup

IIb and non-significant increase in subgroup IIIc versus subgroup IIc.

Body and liver weights (Figure 1b)

Both showed the same statistical results as that of the serum AST.

qRT-PCR results (Figure 1c)

Statistical analysis of ATF-6 showed results like that of the hepatic enzyme.

Hepatic homogenate studies

Colorimetric results

Colorimetric analysis of hepatic TAG & cholesterol results revealed similar statistical results to that of AST (Figure 1d).

ELISA Results

Statistically, levels of the hepatic H₂O₂ & MDA (Figure 1e) were significantly increased in all subgroups than the control group except subgroups IIa & IIIa which showed non-significant increase. Moreover, there was significant increase in subgroups IIb and IIc when compared to subgroups IIa and IIb, respectively. In the recovery group (group III), there was non-significant decrease in subgroup IIIa and IIIb versus subgroups IIa and IIb, correspondingly. However, subgroup IIIc revealed non-significant increase versus IIc. However, the level of TNF- α (Figure 1f) exposed statistical results like that of AST.

On the other hand, the level of GSH (Figure 1f) demonstrated significant decrease in all subgroups versus the control group except subgroups IIa and IIIa. Additionally, there were significant decrease in subgroups IIb and IIc when compared with subgroups IIa and IIb, individually. Moreover, non-significant increase was detected when comparing subgroups IIIa and IIIb with subgroups IIa and IIb, respectively, and non-significant decrease was shown between subgroup IIIc and IIc.

Histological Results

H&E and toluidine blue stained sections

The control group (Figures 2a,bc) revealed ill-defined hexagonal classic hepatic lobules with terminal hepatic venules (THVs) in their centres. The hepatocytes appeared as cords (1 cell-thick) radiating from the THVs, like the spokes of a cartwheel, to the periphery of the hepatic lobules where portal areas were seen. The portal area contained the portal triad embedded in loose connective tissue (CT). This triad was composed of a branch of the bile duct lined with simple cubical epithelium, a branch of the portal vein which had the widest lumen and the thinnest wall and a branch of the hepatic artery with the narrowest lumen.

The hepatocytes appeared as polygonal cells having acidophilic cytoplasm with irregularly pale-stained areas

(representing glycogen deposits) and central large rounded vesicular nuclei with prominent nucleoli. Some cells were binucleated. The cords of the hepatocytes were separated by the blood sinusoids that drained into THVs. The sinusoids were pale spaces lined by endothelial cells (flat & condensed nuclei) and Kupffer cells (ovoid nuclei).

The hepatic sections of FFD for 4 months [subgroup IIa] (Figures 2d,e) demonstrated full picture of steatosis with intracellular fat accumulation as multiple small droplets (microvesicles) and few large droplets pushing the nuclei to one side (macrovesicles). However, FFD for 6 months [subgroup IIb] (Figures 2f,g) resulted in complete image of NASH. There were multiple intracellular fat macrovesicles, hepatocytes ballooning, Mallory-Denk bodies (MDBs, stress-induced proteins and abnormally phosphorylated and cross-linked intermediate keratin filaments, as CK8 and 18), mononuclear inflammatory cell infiltration and marked sinusoidal congestion. In addition, most of the hepatocytes showed either shrunken dense or shrunken irregular nuclei.

Eight months of FFD in subgroup IIc (Figures 2h,i) ensued by appearance of NASH lesion with apparent bridging fibrosis in-between the portal tracts. Such lesion was peppered with multiple small hepatic foci showing dysplastic changes. These dysplastic foci revealed either small cell dysplasia (small cell volume and increased nucleo-cytoplasmic ratio) or large cell dysplasia (large-sized cell with apparently normal nucleo-cytoplasmic ratio [1:1]). Besides, there were nuclear hyperchromasia (salt & pepper chromatin) and increased cytoplasmic density.

The recovery group [group III] revealed regression of the lesion in subgroup IIIa that was not apparent in subgroups IIIb and IIIc. The sections of subgroup IIIa (Figures 2j,k) demonstrated decreased hepatic microvesicular lesion however, the sections of subgroups IIIb and IIIc (Figures 2l,m,n,o) appeared similar to those of subgroups IIb and IIc, respectively.

Masson's trichrome stained sections

Occasional collagen fibers were shown in the portal tracts and around the THVs of the control group and subgroups IIa & IIIa (Figures 3a,b,e). However, the amount of the collagen fibers was increased in subgroups IIb & IIIb (Figures 3c,f) in the same areas. Then it became abundant in NASH areas of subgroups IIc & IIIc (Figures 3d,g) where the collagen fibers appeared bridging between the portal tracts in the interlobular septa.

CYP2E1 immunostained sections

Positive cytoplasmic immunoreaction was noticed in the hepatocytes and the SECs of the control group and subgroups IIa & IIIa (Figures 4a,b,e). In subgroups IIb & IIIb (Figures 4c,f), the reaction spread widely among the hepatocytes and the SECs, then it became extensive in subgroups IIc & IIIc in the hepatocytes and the SECs of the NASH areas and few in the dysplastic foci (Figures 4d,g).

Caspase-3 immunostained sections

The positive immunoreaction was noticed in very few hepatocytes of the control group and subgroups IIa & IIIa (Figures 5a,b,e), then became abundant in most of the hepatocytes and SECs in subgroups IIb & IIIb (Figures 5c,f). In subgroups IIc & IIIc, the positive reaction was dramatically increased in almost all hepatocytes and SECs of NASH areas and completely absent in the cells of the dysplastic foci (Figures 5d,g).

Glypican-3 immunostained sections

There was no immunoreaction in the control group and subgroups IIa, IIb, IIIa and IIIb (the photos were not included). However, few hepatocytes of the dysplastic foci showed positive immunoreaction in subgroups IIc (Figure 6a) and IIIc (Figure 6b).

Morphometric Results

The mean area percent of collagen fibers (Figure 3h), CYP2E1 (Fig. 4h) and caspase-3 (Figure 5h) showed significant increase in all subgroups compared to the control group except subgroups IIa & IIIa which showed non-significant increase. Moreover, there was significant increase in subgroups IIb and IIc versus subgroups IIa and IIb, respectively. In the recovery group (group III), there was non-significant decrease in subgroup IIIa and IIIb versus subgroups IIa and IIb, correspondingly. However, subgroup IIIc revealed non-significant increase versus IIc.

Regarding the mean area percent of glypican-3 immun-expression (Figure 6c), it revealed non-significant increase in subgroup IIIc when compared with subgroup IIc.

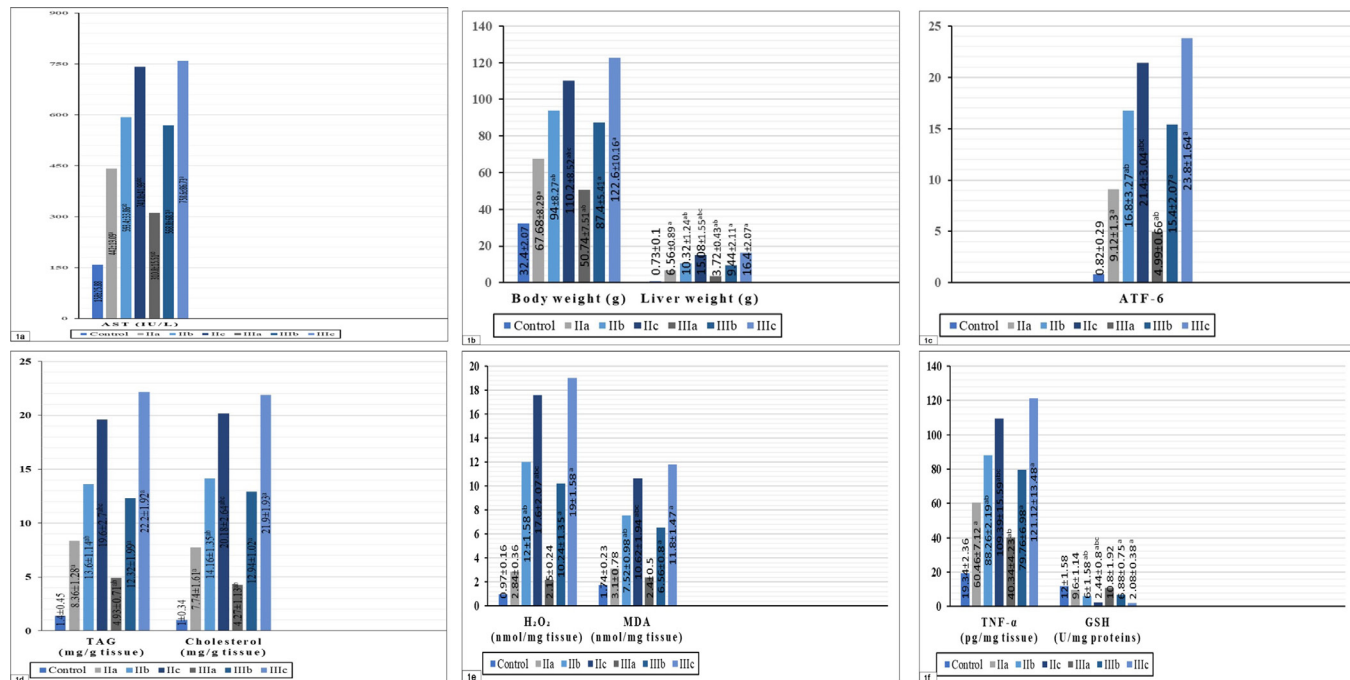


Fig. 1: Illustrating mean values of: (a) serum AST (b) Body and liver weights (c) ATF-6 relative mRNA expression (d) Hepatic TAG & cholesterol (e) Hepatic H₂O₂ & MDA (f) Hepatic TNF-α & GSH. [a, b & c as compared to control group, subgroup IIa & subgroup IIb, respectively (significant difference at $P < 0.05$)]

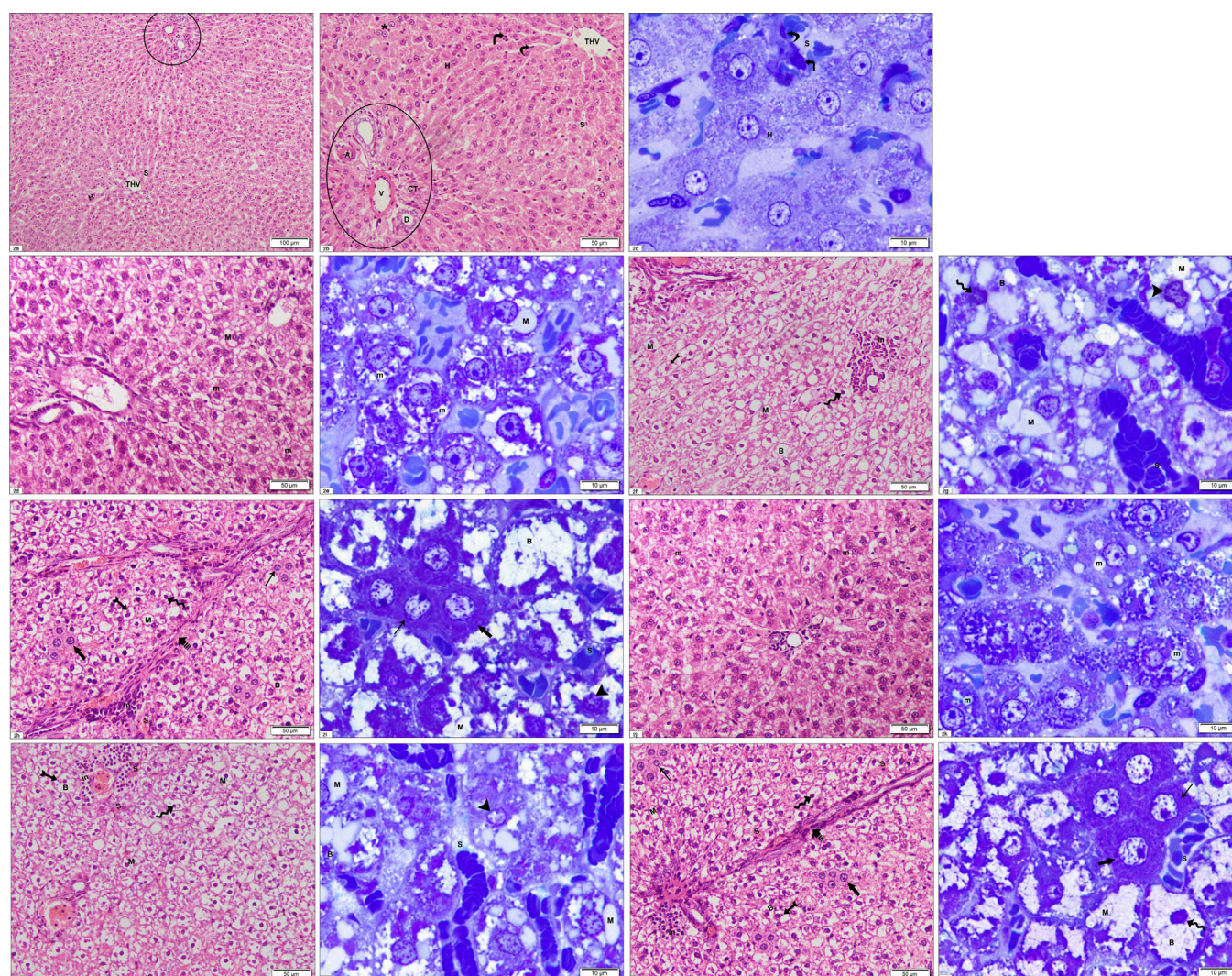


Fig. 2: Photomicrographs of H & E and toluidine blue stained sections of: Control group (a, b & c) showing ill-defined hexagonal classic hepatic lobules, terminal hepatic venules (THV) in their centers, hepatocytes (H) are arranged in cords [1 cell-thick] radiating from the THVs to the periphery of the hepatic lobules - some of them are binucleated (star), in-between the hepatocytes' cords - blood sinusoids (S) are seen lined by endothelial cells (curved arrow) and Kupffer cells (right-angled arrow), portal areas (circled) with loose connective tissue (CT) - a branch of bile duct (D) - a branch of portal vein (V) and a branch of the hepatic artery (A). Subgroup IIa (d & e) showing multiple intracellular microvesicles (m) and few macrovesicles (M). Subgroup IIb (f & g) showing multiple intracellular macrovesicles (M), hepatocyte ballooning (B), hepatocytes with shrunken dense nuclei (wavy arrow), hepatocytes with shrunken irregular nuclei (arrowhead) (Fig. 2g), Mallory-Denk bodies (bifid arrow), mononuclear inflammatory cell infiltration (In), marked sinusoidal congestion (S). Subgroup IIc (h & i) showing areas with M: macrovesicles, B: ballooning, wavy arrow: hepatocytes with shrunken condensed nuclei, arrowhead: hepatocytes with shrunken irregular nuclei (Fig. 2i), bifid arrow: Mallory Denk bodies, In: inflammatory cells, sinusoidal congestion (S), dashed arrow: bridging fibrosis, in addition to scattered small foci with either small cell dysplasia (thin arrow) or large cell dysplasia (thick arrow). Subgroup IIIa (j & k) showing few intracellular microvesicles (m). Subgroup IIIb (l & m) showing M: macrovesicles, B: ballooning, wavy arrow: hepatocytes with shrunken condensed nuclei, arrowhead: hepatocytes with shrunken irregular nuclei (Fig. 2m), bifid arrow: Mallory Denk bodies, In: inflammatory cells, S: congested sinusoids. Subgroup IIIc (n & o) showing areas with M: macrovesicles, B: ballooning, wavy arrow: shrunken condensed nuclei, bifid arrow: Mallory Denk bodies, In: inflammatory cells, sinusoidal congestion (S), dashed arrow: bridging fibrosis, in addition to another areas with small cell dysplasia (thin arrow), and large cell dysplasia (thick arrow). [(H & E, a: x100, b, d, f, h, j, l & n: x200), Toluidine blue, c, e, g, i, k, m & o: x1000]

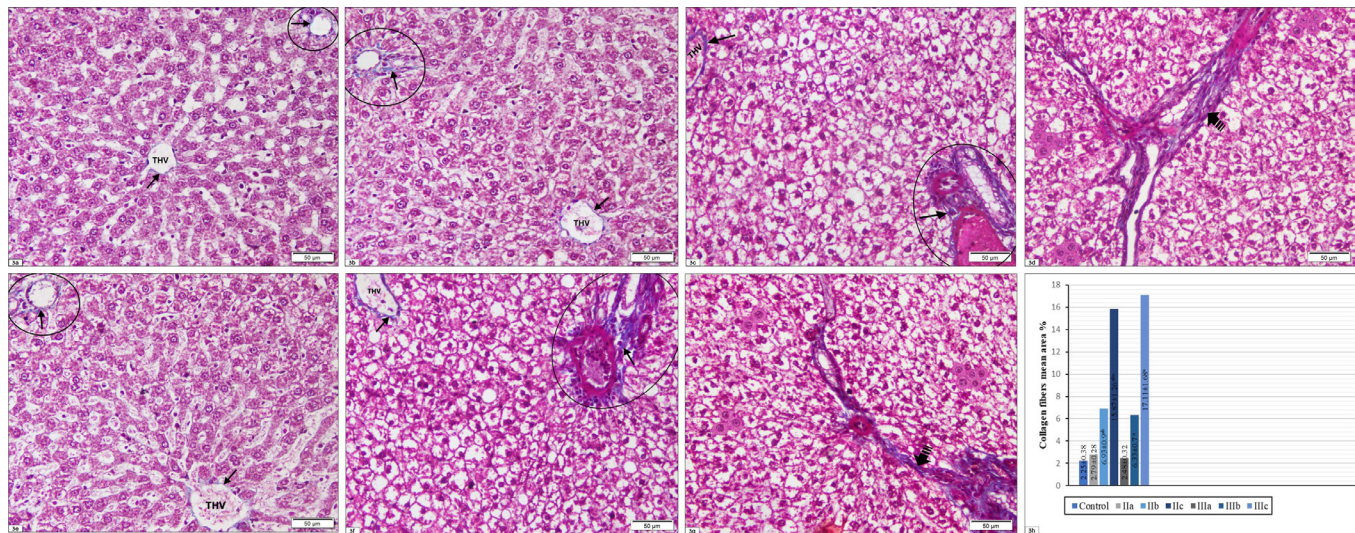


Fig. 3: Photomicrographs of Masson's trichrome stained sections of: Control group, subgroup IIa & subgroup IIIa (a, b & e) showing: occasional collagen fibers (arrow) in the portal tracts (circled) and around the THVs. Subgroup IIb & IIIb (c & f) showing increased amount of the collagen fibers (arrow) in the portal tracts (circled) and around the THVs. Subgroup IIc & IIIc (d & g) showing abundant collagen fibers (dashed arrow) in NASH areas that appeared bridging between the portal tracts in the interlobular septa. [Masson's trichrome, x200] (h) showing mean area % of collagen fibers [a, b & c as compared to control group, subgroup IIa & subgroup IIb, respectively (significant difference at $P < 0.05$)]

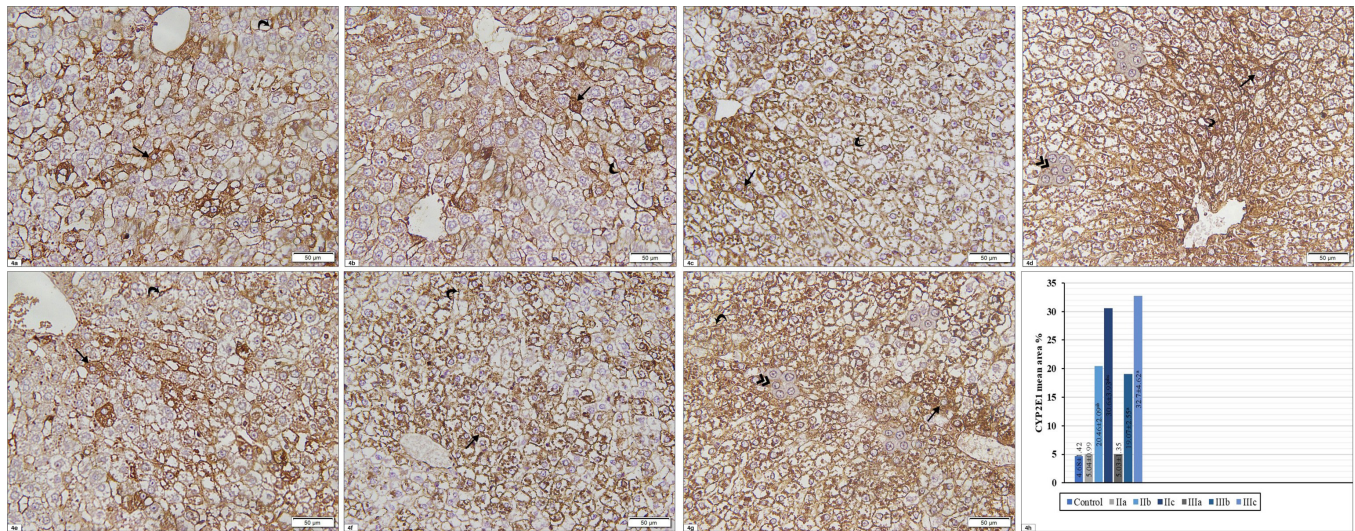


Fig. 4: Photomicrographs of CYP2E1 immunostained sections of: Control group, subgroup IIa & subgroup IIIa (a, b & e) illustrating: positive cytoplasmic immunoreaction in the hepatocytes (arrow) and the SECs (curved arrow). Subgroup IIb & IIIb (c & f) showing widely distributed immunoreaction in the hepatocytes (arrow) and SECs (curved arrow) of the NASH areas and in few cells of the dysplastic foci (double arrowhead). [Immunohistochemical stain for CYP2E1, x200] (h) demonstrating mean area % of CYP2E1 positive immunoreaction [a, b & c as compared to control group, subgroup IIa & subgroup IIb, respectively (significant difference at $P < 0.05$)]

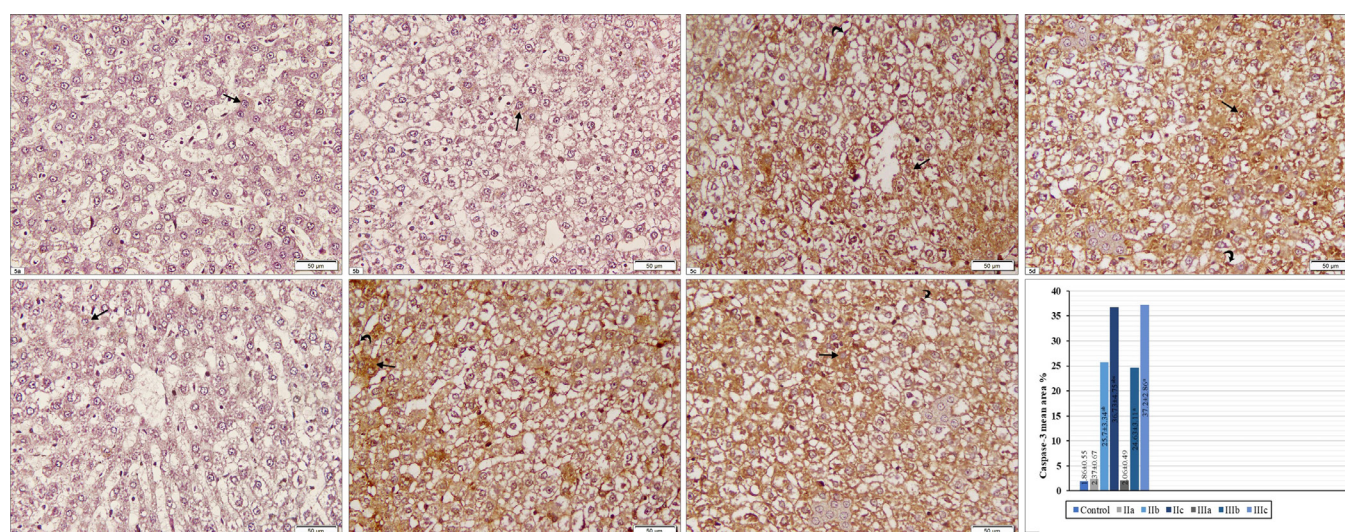


Fig. 5: Photomicrographs of caspase-3 immunostained sections of: Control group, subgroup IIa & subgroup IIIa (a, b & e) illustrating positive immunoreaction in very few hepatocytes (arrow). Subgroup IIb & IIIb (c & f) showing abundant immunoreaction in most of the hepatocytes (arrow) and the SECs (curved arrow). Subgroup IIc & IIIc (d & g) showing dramatic positive immunoreaction in almost all hepatocytes (arrow) and SECs (curved arrow) of NASH areas and negative immunoreaction in the cells of the dysplastic foci. [Immunohistochemical stain for caspase-3, x200] (h) illustrating mean area % of caspase-3 positive immunoreaction [a, b & c as compared to control group, subgroup IIa & subgroup IIb, respectively (significant difference at $P < 0.05$)]

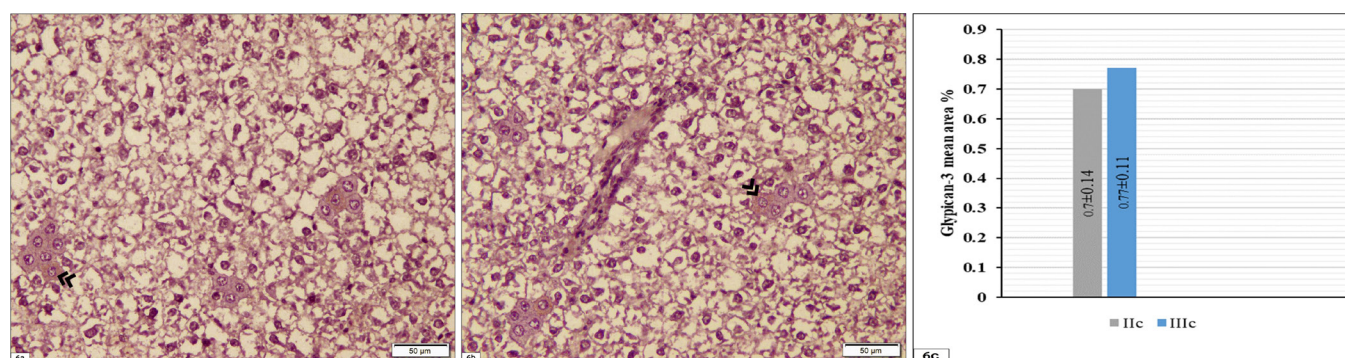


Fig. 6: Photomicrographs of glypican-3 immunostained sections exhibiting positive cytoplasmic immunoreaction (double arrowhead) in few hepatocytes of the dysplastic foci in subgroups IIc and IIIc (a & b) [Immunohistochemical stain for glypican-3, x200] (c) illustrating mean area % of glypican-3 positive immunoreaction

DISCUSSION

This study aimed at evaluating the effects of persistent FFD and sedentary behavior on the hepatic histological and biochemical statuses in adult mice and assessing the possibility of premalignant dysplastic changes with clarifying the role of ER stress and CYP2E1. This was accompanied by highlighting the potentiality of reversing these changes by discontinuation of FFD.

Mice were chosen due to their similarity to human NAFLD regarding its initiation with high caloric intake, hepatic histology, and abnormal metabolism^[27]. Male mice were used as they gained rapid statistically significant increase in the body weight following HFD, in comparison to female ones^[28]. Additionally, estrogens reduce nuclear factor kappa-B (NFκ-B) and subsequently decrease the pro-inflammatory cytokines activation^[29].

Chronic ingestion of FFD [food, in contrast to HFD, has abundant saturated fats, cholesterol and fructose in the soft drinks^[12,13] and sedentary lifestyle for 4 months

(subgroup IIa) increased the body weight significantly than in the control group. This could be elucidated by the excess energy input and diminished energy output^[27,30]. Additionally, there was intra-cytoplasmic hepatic accumulation of lipid micro-droplets which was similarly reported in a former study^[27] following HFD and high fructose and glucose contents of water for 8 weeks. Such finding could be similarly explained by the spillover of the chylomicrons to the liver and ER stress proved to occur by HFD^[7,27,31].

In this subgroup, ER stress was assumed to occur due to increased hepatic synthesis of lipoproteins, that transport the high levels of TAG and cholesterol in blood^[32], beyond ER protein folding capacity^[15]. Also, it could result from high level of SFAs^[33,34] that represent the main fat content of FFD (12%) in this study. As SFAs together with high cholesterol were reviewed to interfere with the normal ER membrane structure (UFAs and low cholesterol). So, they decrease the membrane fluidity and the transport of lipids and newly synthesized proteins across it. Additionally,

SFAs reduce ER calcium store which is important for proper protein folding. This occurs through calcium flux disruption^[15].

In response to ER stress, there is UPR activation (adaptive response) which in turn, induces hepatic lipogenesis [synthesis of TAG and cholesterol from dietary chylomicrons]^[15]. Such ER stress and UPR activation were reinforced in subgroup IIa by the significant increase in the hepatic level of ATF-6 (a UPR activation marker) versus the control group.

Principally, hepatic lipogenesis in this subgroup could occur from dietary chylomicron and de novo from high dietary carbohydrates in FFD^[15]. Such lipogenesis [hepatic fat input] is balanced by mitochondrial β -oxidation and secretion of very low-density lipoprotein-TAG and cholesterol [hepatic fat output]^[31]. However, in this subgroup with continuous intake of high fat content, the rate of fat input was supposed to be more than its output. Such imbalance led to accumulation of TAG and cholesterol in the hepatocytes in the form of microvesicles and the significant increase in their hepatic levels when compared to the control group. This, consequently, led to the significant increase in the liver weight in comparison to that of the control group. Further support came from another studies^[6,8,15,27] where this imbalance resulted in hepatic steatosis and increased serum level of TAG and cholesterol in response to HFD.

Bearing in mind the inflammatory reaction occurred in the adipose tissue following obesity^[30], it could be assumed that deposition of fat in the liver might induce some sort of low-grade inflammation via Kupffer cells stimulation. Such stimulation is followed by pro-inflammatory cytokines release such as TNF- α . This is, consequently, tailed by increased levels of serum hepatic enzymes as AST. This suggestion was supported in subgroup IIa by the significant increase in the levels of hepatic TNF- α and AST than those of the control group.

Continuation of FFD with high loads of SFAs, cholesterol and carbohydrates together with the sedentary lifestyle for 6 months (subgroup IIb) was presumed to result in continued energy budget imbalance. In addition, it was suggested to cause persistent rush of dietary chylomicrons to the liver, continuous ER stress and over-activation of UPR (alarm response), that were similarly reported in former studies^[34,35]. These suppositions were achieved by the significant increase in the body weight and the hepatic levels of ATF-6 versus subgroup IIa.

The over activation of UPR markers in alarm response is followed by NF κ -B inhibitor inactivation with consequent hepatocytes and Kupffer cells' NF κ -B activation. Such activation induces over production of the pro-inflammatory mediators such as TNF- α and interleukin-6 [IL-6]^[36,37]. These events were enforced in subgroup IIb by the significant increase in hepatic level of TNF- α and serum level of the hepatic enzyme (AST) when compared with subgroup IIa. Extra-enforcement came from the spotting of

inflammatory signs in the hepatic sections of this subgroup (dilated congested blood vessels with inflammatory cell infiltration). Besides, the support obtained from earlier studies reporting similar results^[6,27,35].

Basically, ER generates a lot of ROS such as H₂O₂ during protein folding with OS potentiality. This is normally balanced by the antioxidants activated by UPR^[16,20]. With high protein folding and ER stress in subgroup IIb, there was marked OS due to increase in ROS production over the antioxidant capacity, especially that of GSH which was reported to decrease by high fat diet^[20]. This was confirmed by the significant increase in hepatic level of H₂O₂ and significant decrease in that of GSH in this subgroup versus subgroup IIa. Consequently, the increase in OS increases ER stress producing a vicious circle between ER stress and OS^[38].

The alarm response of the UPR was reported to progress to apoptosis response where UPR fails to ameliorate the marked continuous ER stress^[15]. This occurs through UPR markers-induced CHOP (pro-apoptotic protein) expression^[27,35]. Moreover, calcium efflux from ER and its influx to the mitochondria through tethers linking smooth and rough ER with mitochondria^[39] cause increased mitochondrial membrane permeability and cytochrome-C release with subsequent initiation of intrinsic apoptotic pathway^[27,40]. Furthermore, activation of Fas ligand and receptors during NASH progression initiates the extrinsic apoptotic pathway^[41]. Such apoptosis was supported in subgroup IIb by the presence of apoptotic features in the hepatocytes and the significant increase in the mean area percent of caspase-3 immunoreaction in this subgroup versus subgroup IIa.

Furtherly, there were MDBs (abnormally phosphorylated and cross-linked intermediate keratin filaments, as CK8 and 18) in the hepatocytes in this subgroup. These bodies were reported to be a sign of inflammation and a factor that increases the hepatocytes susceptibility to apoptosis^[42].

In addition, there was detection of caspase-3 immunoreaction in the SECs of this subgroup. Such SEC apoptosis was explained previously by the activation of membranous Fas induced by high amount of fatty acids passing through them from the blood to the liver in NASH. Although the SECs, under the normal conditions, resist the effect of Fas, they become sensitive to it in cases of NASH due to the high level of TNF- α documented in this study and in a former study^[43].

The altered SECs activate Kupffer cells that, in turn, produce pro-inflammatory mediators which add to the detected inflammation in this subgroup. In addition, they induce hepatic stellate cells (HSCs) activation with the subsequent fibrosis due to distorted SECs shield separating the HSCs in the peri-sinusoidal areas form the high level of fats in the sinusoidal lumens^[4,6,27,31,35,44]. These consequences could illuminate the fibrosis verified in subgroup IIb via the significant increase in the collagen fibers area percent in this subgroup versus subgroup IIa.

Moreover, over-activation of UPR markers induces insulin resistance via activation of c-Jun-NH2-terminal kinase [JNK] that induces and aggravates apoptosis in this subgroup^[45]. In addition, JNK obstructs insulin signalling by interfering with the proper function of insulin receptors^[35,45]. The insulin resistance increases lipolysis in the adipose tissue and lipogenesis in the liver^[46,47].

Consequently, the high level of lipogenesis (de novo from excess carbohydrates, hepatic from dietary chylomicrons rush and hepatic from free fatty acids produced by insulin resistance-induced lipolysis) together with mitochondrial dysfunction and decreased β -oxidation resulted in extensive accumulation of TAG and cholesterol in the liver. This was backed by the significant increase in their hepatic levels and in the liver weight in subgroup IIb versus subgroup IIa, in addition to the wide presence of macrovesicles in liver sections. Similar results were recorded formerly in response to treatment with high levels of SFAs and UFAs^[7,27].

Unsurprisingly, subgroup IIb revealed significant increase in CYP2E1 immunoreaction area percent in the hepatocytes and the SECs when compared to that in subgroup IIa. This increase in ω -1 hydroxylation of the SFAs occurred as an alternative pathway to the decrease in their β -oxidation^[19,20] that occurred in this subgroup, especially with the high levels of SFAs. Moreover, ER stress-induced insulin resistance with high serum glucose and insulin levels led to increased production of ketone bodies which sequentially increase CYP2E1 level^[20].

ω -1 hydroxylation of the high levels of SFAs results in production of large amounts of ROS in hepatocytes and SECs such as superoxide anion and H₂O₂^[16,48] that is followed by lipid peroxidation, protein denaturing and DNA and RNA damage^[16,19,20]. Lipid peroxidation produces intermediate products (fatty acid radicals and lipid peroxides) and finally produces reactive aldehydes [MDA & 4-hydroxynonenal (HNE)]^[49]. Such lipid peroxidation, in the mitochondria, with its lipid intermediates and the final products (MDA & HNE) results into their dysfunction with subsequent release of more ROS, especially H₂O₂, and release of cytochrome-C with resultant apoptosis of hepatocytes and SECs^[48]. These events were backed by the significant increase in the level of hepatic MDA in subgroup IIb versus subgroup IIa. Additionally, they added to the explanation of the significant increase in the hepatic levels of H₂O₂ and in the area percent of caspase-3 immunoreaction occurred in subgroup IIb.

Chronic and persistent ingestion of FFD with an inactive lifestyle in subgroup IIc was believed to induce progression and exaggeration of the whole hepatic lesions, as documented previously^[27,50]. Such expectation was defended by the significant increase in the body and liver weights in this subgroup versus subgroup IIb, in addition to all biochemical markers in the serum and liver homogenates, except hepatic GSH that showed significant decrease. Additionally, there was significant increase in

the area percent of collagen fibers, CYP2E1 and caspase-3 immunoreaction in subgroup IIc compared to subgroup IIb.

Astonishingly, subgroup IIc disclosed multiple small dysplastic foci (altered regeneration foci) in the liver sections. Such result was reinforced by the appearance of few glypican-3 positive immune-activity. Further support came from a previous study that reported positive glypican-3 immunoreaction in about 9% of the dysplastic cells^[51]. These dysplastic changes could be explained by the high levels of reactive aldehydes resulted from intensive ω -1 hydroxylation. As these products were proved to be mutagenic and carcinogenic where they react with DNA forming DNA adducts (DNA segments attached to oncogenic chemical)^[52].

The recovery group of this study (group III) exposed significant improvement of all histological and biochemical signs of steatosis in subgroup IIIa versus subgroup IIa. This improvement was anticipated based on a previous study^[7] that stated rapid recovery of hepatic steatosis on stoppage of the initiating factors. Despite this expectation, the improvement did not reach the control parameters as it might need more time to achieve the proper recovery.

However, in subgroup IIIb, there was poor recovery where all histological and biochemical parameters were not significantly improved than those in subgroup IIb. This finding was supported by an earlier study^[53] where OC or even diet with low fat and cholesterol for 2 months have restricted ability to reverse NASH lesions induced by 6 months of fast-food diet. Moreover, in subgroup IIIc there was no detection of any improvement since all the histological and the biochemical findings showed slight worsening with no significant deterioration than those in subgroup IIc. This finding might suggest the incapacity of recovery from dysplasia and the possibility of its progression to HCC with time which was stated to occur in some cases^[27,50,54].

It could be concluded that chronic ingestion of FFD with sedentary lifestyle can be considered as triggering factors for hepatic steatosis that may progress to NASH with persistence of these factors. These hepatic lesions could occur via ER stress, activation of UPR and over expression of CYP2E1 that increase with continuation of the precipitating factors. With time, this hepatic insult may progress to dysplasia which is a warning sign for HCC development. Additionally, easy recovery of the hepatic steatosis, poor recovery of NASH and no recovery of dysplasia were concluded, however, more time might be needed to achieve proper judgement on the state of recovery.

CONFLICT OF INTERESTS

There are no conflicts of interest.

REFERENCES

1. Bray F, Ferlay J, Soerjomataram I, Siegel RL, Torre LA, Jemal A. Global cancer statistics 2018: GLOBOCAN estimates of incidence and mortality worldwide for 36 cancers in 185 countries. *CA Cancer J Clin* 2018; 68: 394-424.
2. Tabrizian P, Jibara G, Shrager B, Schwartz M, Roayaie S. Recurrence of hepatocellular cancer after resection: patterns, treatments, and prognosis. *Ann Surg*. 2015; 261:947-55.
3. Park YN. Update on precursor and early lesions of hepatocellular carcinomas. *Arch Pathol Lab Med*. 2011; 135:704-15.
4. Newell P, Villanueva A, Friedman SL, Koike K, Llovet JM. Experimental models of hepatocellular carcinoma. *J Hepatol*. 2008; 48: 858-79.
5. Bellentani S. The epidemiology of non-alcoholic fatty liver disease. *Liver Int*. 2017; 37 1:81-4.
6. Carvajal S, Perramón M, Oró D, Casals E, Fernández-Varo G, Casals G, Parra M, González de la Presa B, Ribera J, Pastor Ó, Morales-Ruiz M, Puentes V, Jiménez W. Cerium oxide nanoparticles display antilipogenic effect in rats with non-alcoholic fatty liver disease. *Sci Rep*. 2019; 9:12848.
7. Parafati M, Kirby RJ, Khorasanizadeh S, Rastinejad F, Malany S. A nonalcoholic fatty liver disease model in human induced pluripotent stem cell-derived hepatocytes, created by endoplasmic reticulum stress-induced steatosis. *Dis Model Mech*. 2018; 11: dmm033530.
8. Bedossa P. Pathology of non-alcoholic fatty liver disease. *Liver Int*. 2017; 37:85-9.
9. Lian CY, Zhai ZZ, Li ZF, Wang L. High fat diet-triggered non-alcoholic fatty liver disease: A review of proposed mechanisms. *Chem Biol Interact*. 2020; 330:109199.
10. Charlton M, Krishnan A, Viker K, Sanderson S, Cazanave S, McConico A, Masuoko H, Gores G. Fast food diet mouse: novel small animal model of NASH with ballooning, progressive fibrosis, and high physiological fidelity to the human condition. *Am J Physiol Gastrointest Liver Physiol*. 2011; 301: G825-34.
11. Pydyn N, Miękus K, Jura J, Kotlinowski J. New therapeutic strategies in nonalcoholic fatty liver disease: a focus on promising drugs for nonalcoholic steatohepatitis. *Pharmacol Rep*. 2020; 72:1-12.
12. Bashir AI, Sma S, Ahmed MQ, Mansi MH, Dheem RY, AI A, Aied M, Alanzy H, Msekohay A, Alrshedy O, Majeed A, Mesnad A, Shammari A. Study on the effects of fast food on the glucose and lipid profile aims to provide a platform to advocate a healthier lifestyle and better eating habits. *Journal of Pharmaceutical and Biological Science*. 2017; 5:175-8.
13. Basaranoglu M, Basaranoglu G, Sabuncu T, Sentürk H. Fructose as a key player in the development of fatty liver disease. *World J Gastroenterol*. 2013; 28: 1166-72.
14. Lee JS, Zheng Z, Mendez R, Ha SW, Xie Y, Zhang K. Pharmacologic ER stress induces non-alcoholic steatohepatitis in an animal model. *Toxicol Lett*. 2012; 20: 29-38.
15. Gentile CL, Frye M, Pagliassotti MJ. Endoplasmic reticulum stress and the unfolded protein response in nonalcoholic fatty liver disease. *Antioxid Redox Signal*. 2011; 15: 505-21.
16. Lu Y, Cederbaum AI. CYP2E1 and oxidative liver injury by alcohol. *Free Radic Biol Med*. 2008; 44:723-38.
17. Yasuko I. Alcohol metabolism in liver sinusoidal endothelial cells. NIH 2016. R21-AA023599-01A1.
18. Stoyanova T, Lessigiarska I, Mikov M, Pajeva I, Yanev S. Xanthates As Useful Probes for Testing the Active Sites of Cytochromes P450 4A11 and 2E1. *Front Pharmacol*. 2017; 8:672.
19. Xu J, Ma HY, Liang S, Sun M, Karin G, Koyama Y, Hu R, Quehenberger O, Davidson NO, Dennis EA, Kisseleva T, Brenner DA. The role of human cytochrome P450 2E1 in liver inflammation and fibrosis. *Hepatol Commun*. 2017; 1:1043-57.
20. Leung TM, Nieto N. CYP2E1 and oxidant stress in alcoholic and non-alcoholic fatty liver disease. *J Hepatol*. 2013; 58:395-8.
21. El-Sherif, Mohamed Wefky. Optimization of Xylazine-Ketamine Anesthetic Dose in Mice with Chronic Liver Injury. *Acad. J. Biolog. Sci. (B. Zoology)* 2019; 11(1): 13-18.
22. El Agaty SM. Cardioprotective effect of vitamin D2 on isoproterenol-induced myocardial infarction in diabetic rats. *Archives of Physiology and Biochemistry* 2019; 125:210-19.
23. Kiernan JA. *Histological and histochemical methods: Theory and practice*. 5th ed, Scion Publishing, Banbury, UK. 2015; pp. 111-62.
24. Suvarna K, Layton C, Bancroft J. *Connective and mesenchymal tissue with their stains. Immunohistochemical techniques* In: Bancroft's *Theory and practice of Histological Techniques*, 7th ed, Churchill Livingstone Elsevier, Oxford. 2013; pp. 187-214, 381-426.
25. Hayat MA. *Chemical fixation*. In: *Principles and techniques of electron microscopy: biological applications*. 4th ed. Edinburg, UK: Cambridge University Press. 2000; pp. 4-85.
26. Emsley R, Dunn G, White IR. Mediation and moderation of treatment effects in randomised controlled trials of complex interventions. *Stat Methods Med Res* 2010; 19: 237-70.

27. Asgharpour A, Cazanave SC, Pacana T, Seneshaw M, Vincent R, Banini BA, Kumar DP, Daita K, Min HK, Mirshahi F, Bedossa P, Sun X, Hoshida Y, Koduru SV, Contaifer D Jr, Warncke UO, Wijesinghe DS, Sanyal AJ. A diet-induced animal model of non-alcoholic fatty liver disease and hepatocellular cancer. *J Hepatol.* 2016; 65:579-88.
28. Recena Aydos L, Aparecida do Amaral L, Serafim de Souza R, Jacobowski AC, Freitas Dos Santos E, Rodrigues Macedo ML. Nonalcoholic Fatty Liver Disease Induced by High-Fat Diet in C57bl/6 Models. *Nutrients.* 2019; 11:3067.
29. Wands J. Hepatocellular carcinoma and sex. *N Engl J Med.* 2007; 357:1974-6.
30. Kim OK, Jun W, Lee J. Mechanism of ER Stress and Inflammation for Hepatic Insulin Resistance in Obesity. *Ann Nutr Metab.* 2015; 67:218-27.
31. Koo SH. Nonalcoholic fatty liver disease: molecular mechanisms for the hepatic steatosis. *Clin Mol Hepatol.* 2013; 19:210-5.
32. Jo H, Choe SS, Shin KC, Jang H, Lee JH, Seong JK, Back SH, Kim JB. Endoplasmic reticulum stress induces hepatic steatosis via increased expression of the hepatic very low-density lipoprotein receptor. *Hepatology.* 2013; 57:1366-77.
33. Fuchs M, Sanyal AJ. Lipotoxicity in NASH. *J Hepatol.* 2012; 56:291-3.
34. Leamy AK, Egnatchik RA, Young JD. Molecular mechanisms and the role of saturated fatty acids in the progression of non-alcoholic fatty liver disease. *Prog Lipid Res.* 2013; 52:165-74.
35. Velázquez KT, Enos RT, Bader JE, Sougiannis AT, Carson MS, Chatzistamou I, Carson JA, Nagarkatti PS, Nagarkatti M, Murphy EA. Prolonged high-fat-diet feeding promotes non-alcoholic fatty liver disease and alters gut microbiota in mice. *World J Hepatol.* 2019; 11:619-37.
36. Liu X, Green RM. Endoplasmic reticulum stress and liver diseases. *Liver Res.* 2019; 3:55-64.
37. Hop HT, Reyes AWB, Huy TXN, Arayan LT, Min W, Lee HJ, Rhee MH, Chang HH, Kim S. Activation of NF- κ B-Mediated TNF-Induced Antimicrobial Immunity Is Required for the Efficient *Brucella abortus* Clearance in RAW 264.7 Cells. *Front Cell Infect Microbiol.* 2017; 7:437.
38. Cao SS, Kaufman RJ. Endoplasmic reticulum stress and oxidative stress in cell fate decision and human disease. *Antioxid Redox Signal.* 2014; 21:396-413.
39. Vallese F, Barazzuol L, Maso L, Brini M, Cali T. ER-Mitochondria Calcium Transfer, Organelle Contacts and Neurodegenerative Diseases. *Adv Exp Med Biol.* 2020; 1131:719-46.
40. Sunny NE, Bril F, Cusi K. Mitochondrial adaptation in Nonalcoholic Fatty Liver Disease: Novel Mechanisms and Treatment Strategies. *Endocrinol. Metab.* 2017; 28: 250-60.
41. Alkhouri N, Alisi A, Okwu V, Matloob A, Ferrari F, Crudele A, De Vito R, Lopez R, Feldstein AE, Nobili V. Circulating Soluble Fas and Fas Ligand Levels Are Elevated in Children with Nonalcoholic Steatohepatitis. *Dig Dis Sci.* 2015; 60:2353-9.
42. Maher MM, Ibrahim WA, Saleh SA, Shash L, Abou Gabal H, Tarif M, Gamal M. Cytokeratin 18 as a non invasive marker in diagnosis of NASH and its usefulness in correlation with disease severity in Egyptian patients. *The Egyptian Journal of Medical Human Genetics* 2015; 16: 41-6.
43. Cardier JE, Erickson-Miller CL. Fas (CD95)- and tumor necrosis factor-mediated apoptosis in liver endothelial cells: role of caspase-3 and the p38 MAPK. *Microvasc Res.* 2002; 63:10-8.
44. Miyao M, Kotani H, Ishida T, Kawai C, Manabe S, Abiru H, Tamaki K. Pivotal role of liver sinusoidal endothelial cells in NAFLD/NASH progression. *Lab Invest.* 2015; 95:1130-44.
45. García-Monzón C, Lo Iacono O, Mayoral R, *et al.* Hepatic insulin resistance is associated with increased apoptosis and fibrogenesis in nonalcoholic steatohepatitis and chronic hepatitis C. *J Hepatol.* 2011; 54:142-52.
46. Morigny P, Houssier M, Mouisel E, Langin D. Adipocyte lipolysis and insulin resistance. *Biochimie.* 2016; 125:259-66.
47. Smith GI, Shankaran M, Yoshino M, *et al.* Insulin resistance drives hepatic de novo lipogenesis in nonalcoholic fatty liver disease. *J Clin Invest.* 2020; 130:1453-60.
48. García-Suástegui WA, Ramos-Chávez LA, Rubio-Osornio M, Calvillo-Velasco M, Atzin-Méndez JA, Guevara J, Silva-Adaya D. The Role of CYP2E1 in the Drug Metabolism or Bioactivation in the Brain. *Oxid Med Cell Longev.* 2017; 2017:4680732.
49. Ayala A, Muñoz MF, Argüelles S. Lipid peroxidation: production, metabolism, and signaling mechanisms of malondialdehyde and 4-hydroxy-2-nonenal. *Oxid Med Cell Longev.* 2014; 2014:360438.
50. Younossi ZM, Otgonsuren M, Henry L, Venkatesan C, Mishra A, Erario M, Hunt S. Association of nonalcoholic fatty liver disease (NAFLD) with hepatocellular carcinoma (HCC) in the United States from 2004 to 2009. *Hepatology* 2015; 62: 1723-30.
51. Di Tommaso L, Franchi G, Park YN, Fiamengo B, Destro A, Morengi E, Montorsi M, Torzilli G, Tommasini M, Terracciano L, Tornillo L, Vecchione R, Roncalli M. Diagnostic value of HSP70, glypican 3, and glutamine synthetase in hepatocellular nodules in cirrhosis. *Hepatology.* 2007; 45:725-34.

52. Seitz HK, Wang XD. The role of cytochrome P450 2E1 in ethanol-mediated carcinogenesis. *Subcell Biochem.* 2013; 67:131-43.
53. Lytle KA, Jump DB. Is Western Diet-Induced Nonalcoholic Steatohepatitis in Ldlr^{-/-} Mice Reversible? *PLoS One.* 2016 13;11: e0146942.
54. Dongiovanni P, Romeo S, Valenti L. Hepatocellular carcinoma in nonalcoholic fatty liver: role of environmental and genetic factors. *World J Gastroenterol.* 2014; 20:12945-55.

الملخص العربي

عواقب الوجبات السريعة من التنكس الدهني الكبدي إلى خلل التنسج في الفئران الذكور البالغة غير النشطة مع تسليط الضوء على أدوار إجهاد الشبكة الإندوبلازمية والبروتين الصبغي الخلوي ب ٤٥٠ عائلة ٢ فصيلة ه وإمكانية التعافي

عبير إبراهيم عبد اللاه عمر، مروة محمد يسري، ايمان عباس فرج

قسم الهستولوجي، كلية الطب، جامعة القاهرة، مصر

الخلفية: يعتبر مرض الكبد الدهني غير الكحولي سبب شائع لأمراض الكبد المزمنة على مستوى العالم. يصيب ٢٠-٤٠٪ من السكان و ٧٠-٩٥٪ من مرضى السكري والسمنة. ويمكن أن يتطور مرض الكبد الدهني غير الكحولي من التنكس الدهني الكبدي إلى التهاب الكبد الدهني غير الكحولي. وقد انتشر استخدام نظام غذاء الوجبات السريعة كنظام غذائي على نطاق واسع في جميع أنحاء العالم نظرًا لسهولة استخدامه واستساغته.

الهدف من العمل: هدفت هذه الدراسة إلى تقييم التغيرات الكبدية النسيجية والكيميائية الحيوية التي حدثت في ذكور الفئران البالغة على نظام غذاء الوجبات السريعة المستمر ونمط الحياة الخامل ، وأيضاً دراسة إمكانية حدوث تغيرات ما قبل السرطان من خلل التنسج ، وإمكانية الشفاء بعد توقف نظام غذاء الوجبات السريعة. علاوة على ذلك ، تم تقييم الدور المحتمل لإجهاد الشبكة الإندوبلازمية والبروتين الصبغي الخلوي ب ٤٥٠ عائلة ٢ فصيلة ه.

المواد وطرق البحث: تم الاحتفاظ ب ٤٨ فأر ذكر بالغ منفردة في أقفاص ، وتم تقسيمها إلى المجموعات الضابطة ، ومجموعة غذاء الوجبات السريعة، ومجموعة التعافي. كما تم تقسيم كل مجموعة وفقاً لوقت التضحية. تم التضحية ب ٣ من المجموعات الفرعية الضابطة مع مجموعات غذاء الوجبات السريعة الفرعية عند ٤ و ٦ و ٨ أشهر. بينما تم التضحية بالثلاث مجموعات الفرعية الضابطة المتبقية مع مجموعات التعافي الفرعية عند ٦ و ٨ و ١٠ أشهر. وتم إجراء الدراسات الكيميائية الحيوية والنسيجية والقياسات المترية الشكلية.

النتائج: أظهرت مجموعة نظام غذاء الوجبات السريعة إصابات كبدية متزايدة بدءاً من تراكم الحويصلات الدهنية الصغيرة إلى ترسب الحويصلات الكبيرة مع إجهاد الشبكة الإندوبلازمية ، وتنشيط استجابة البروتينات الغير مطوية ، وزيادة ضخمة في البروتين الصبغي الخلوي ب ٤٥٠ عائلة ٢ فصيلة ه ، والالتهابات ، وموت الخلايا المبرمج. ثم كان هناك تطور لبؤر صغيرة متعددة من خلل التنسج في المنطقة المصابة. كان التحسن في مجموعة التعافي ذو دلالة إحصائية في حالة التنكس الدهني الكبدي ، وبدون دلالة إحصائية في حالة التهاب الكبد الدهني غير الكحولي، وغير موجود في خلل التنسج.

الاستنتاج: يمكن أن يؤدي نظام غذاء الوجبات السريعة المزمن المصاحب لنمط الحياة الخاملة إلى التنكس الدهني الكبدي والذي يتبع بالتهاب الكبد الدهني غير الكحولي من خلال إجهاد الشبكة الإندوبلازمية ، وتفعيل استجابة البروتينات الغير مطوية، والتنشيط المفرط للبروتين الصبغي الخلوي ب ٤٥٠ عائلة ٢ فصيلة ه. وقد تتطور الإصابة مع استمرار نظام غذاء الوجبات السريعة والسلوك غير النشط إلى خلل التنسج ، وهو إصابة قابلة للتسرب. وعلى الرغم من الحاجة إلى مزيد من الوقت لإجراء تقييم مناسب للتعافي ، إلا أنه يمكن افتراض أن التنكس الدهني الكبدي يمكن التعافي منه بسهولة ، وأن التهاب الكبد الدهني غير الكحولي غير قابل للتعافي بشكل جيد بينما يكون خلل التنسج غير قابل للتعافي.